

yield are influenced by the explanatory variables included in the model. It is evident from the data that human labour, seed and nursery raising, manure and fertilizer, and transport charges show positive and significant impact on crop production. Hence, increase in inputs such as human labour, seed, nursery, manure, fertilizer and transport would influence the crop yield.

*A. annua* crop has been introduced by CSIR-CIMAP in India under contractual cultivation and buy-back arrangement with pharma industries to avoid marketing problems for the farmers. In the study areas in UP contractual cultivation is being done by the M/s Ipcra Laboratories, Ratlam from 2009 onwards; the whole produce is purchased by the company directly from the farmers at a price mutually agreed to by both of them before planting the crop. Farmers are cultivating this crop on the basis of contractual cultivation guided by CSIR-CIMAP. However, the major constraints faced by farmers in producing the crop include shortage of labour in harvesting and threshing season, absence of input subsidies and poor access to loan from

banks, shortage of electricity, lack of regulated market, lack of storage and drying facilities.

The present study shows that cultivation of *A. annua* provides high returns to farmers in a short span of about four months. The contractual cultivation under PPP model strengthens the farmers to adopt new technologies and crops. It is concluded from the study, that cultivation of industrial/medicinal crops under contractual cultivation will give a boost for expansion of new crops by providing assured returns to the farmers and avoiding the marketing problems and price-lowering during peak harvest season.

1. CSIR-CIMAP technology bulletin *Artemisinin* production from *Artemisia annua*: technology package, 2005, 1.
2. Dhawan, S., Pal, A. and Kumar, S., Abstract book of National Workshop on Innovation and Technology Transfer to Industries: Role of Universities, Babasaheb Bhimrao Ambedkar University, Lucknow, 10 and 11 March 2014, p. 23.
3. Kumar, S., Suresh, R., Singh, V. and Singh, A. K., *Agric. Econ. Res. Rev.*, 2011, 24, 346–350.

4. Suresh, R., Kumar, S., Singh, V., Pravesh, R., Tomar, V. K. S. and Singh, A. K., *Agric. Econ. Res. Rev.*, 2012, 25, 157–160.
5. Ellman, A., *Outlook on Pest Management*, April 2010, pp. 84–88.

ACKNOWLEDGEMENT. We thank the Director, CSIR-CIMAP, Lucknow for guidance and support during the study.

Received 18 August 2014; revised accepted 13 July 2015

SANJAY KUMAR<sup>1,\*</sup>  
RAM SURESH<sup>1</sup>  
DEEPAK KUMAR VERMA<sup>1</sup>  
ALKA DANGESH<sup>2</sup>  
V. K. S. TOMAR<sup>1</sup>

<sup>1</sup>Technology and Business Development Division,  
CSIR-Central Institute of Medicinal and Aromatic Plants,  
Lucknow 226 015, India  
<sup>2</sup>Ipcra Laboratories Limited,  
Ratlam 457 002, India  
\*For correspondence.  
e-mail: sanjaykumar@cimap.res.in

## An approach to improve shallow surface investigation using joint analysis of Rayleigh and Love waves

Rayleigh and Love waves travel along the surface and are commonly characterized by relatively low velocity, low frequency and high amplitude<sup>1</sup>. Longer wavelengths penetrate greater depths and exhibit greater phase velocities, and are more sensitive to the elastic properties of the deeper layers<sup>2</sup>. On the contrary, shorter wavelengths are more sensitive to the physical properties of shallow surface layers. The particle motion for the fundamental mode of Rayleigh waves in a homogeneous medium is elliptical in a counter-clockwise (retrograde) direction along the free surface<sup>3</sup>. With depth, the particle motion turns out to be prograde and is elliptical when reaching appropriate depth. The dispersive properties of Rayleigh wave for near-surface characterization have been well-established<sup>3–9</sup>. Love wave is generated from the total internal and multiple reflections of horizontally polarized shear wave (SH)<sup>10</sup>.

The dispersion properties of Love wave are independent of *P*-wave velocity<sup>11</sup>, thus, it gives a clear inverted *S*-wave velocity model.

Joint analysis of Rayleigh and Love waves dispersion is accomplished to improve the vertical shear wave velocity ( $V_S$ ) profiles. If the energy of all modes is not considered accurately, it leads to ambiguous or erroneous subsurface velocity models. Non-uniqueness is a well-known issue that affects most of geophysical techniques<sup>12,13</sup>. However, the non-uniqueness of the solution<sup>14,15</sup> can be resolved by performing the inversion

using prior geological information of the area. Therefore, joint analysis of dispersive properties for both the Rayleigh and Love waves could be used as a highly valuable tool in the improvement of subsurface investigation<sup>16</sup>.

In the present study the data have been acquired over upper ground, Indian School of Mines, Dhanbad using the 24-channel Stratavizor NZ seismograph with 4.5 Hz vertical and horizontal geophones for understanding the potential usefulness of joint analysis of Rayleigh and Love wave dispersion to improve vertical shear wave velocity distribution in

**Table 1.** Summary of field data acquisition

Recorded component	Source	Type of geophone	Orientation of geophone
Vertical component of Rayleigh wave ( <i>P</i> )	Vertical	Vertical (4.5 Hz)	Vertically inserted
Love wave (SH)	Horizontal	Horizontal	Perpendicular to the array

shallow surface investigations. The data recording has been conducted using 4.5 Hz vertical geophones by vertical impact with 15 kg wooden hammer. Whereas 4.5 Hz horizontal geophones have been implanted at the same location corresponding to each 4.5 Hz vertical geophones location and the wooden hammer has been used by horizontal impact at an edge of a wooden log fixed on the ground. The sampling interval is taken 0.25 ms, and record lengths as 1 sec. The vertical component of Rayleigh ( $P$ ) and Love waves (SH) has been picked for a fixed geophone spread location with different configuration as summarized in Table 1.

The acquired data have been preprocessed for preserving the useful surface wave part while removing the refraction part from them. The surface wave components are then enhanced using high cut filter by removing phases above 60 Hz. The surface waves phase below 60 Hz is utilized for velocity spectrum generation. Different modes (fundamental mode and all higher possible modes) of the vertical component of Rayleigh and Love waves are picked for the generation of corresponding dispersion curves. The extracted dispersion curves of Rayleigh and Love waves for all the modes have been inverted separately and then jointly using genetic algorithm (GA)<sup>16</sup>. Most geophysical modelling problems are traditionally solved using local optimization techniques, such as linearized matrix inversion, steepest descent, conjugate gradients or grid search techniques. These techniques sometimes converge to a local minima and depend strongly on the starting model. A global optimization technique such as GA diminishes these problems and is an attractive search tool suitable for the irregular multimodal fitness functions typically observed in seismic modelling. In GA, a series of ‘genetic operations’ (namely selection, crossover and mutation) act along various successive steps (generations) to minimize (or maximize) a certain fitness function that measures how good a certain model is with respect to a desired characteristic<sup>17,18</sup>. In the present study, acquired data have been processed using WinMASW 6.2, ELIOSOFT software.

The refracted  $P/S$  waves were removed and further processed using 60 Hz high cut filter to enhance the surface waves. Figure 1 *a* and *b* shows the enhanced 24-channel seismic trace corresponding to

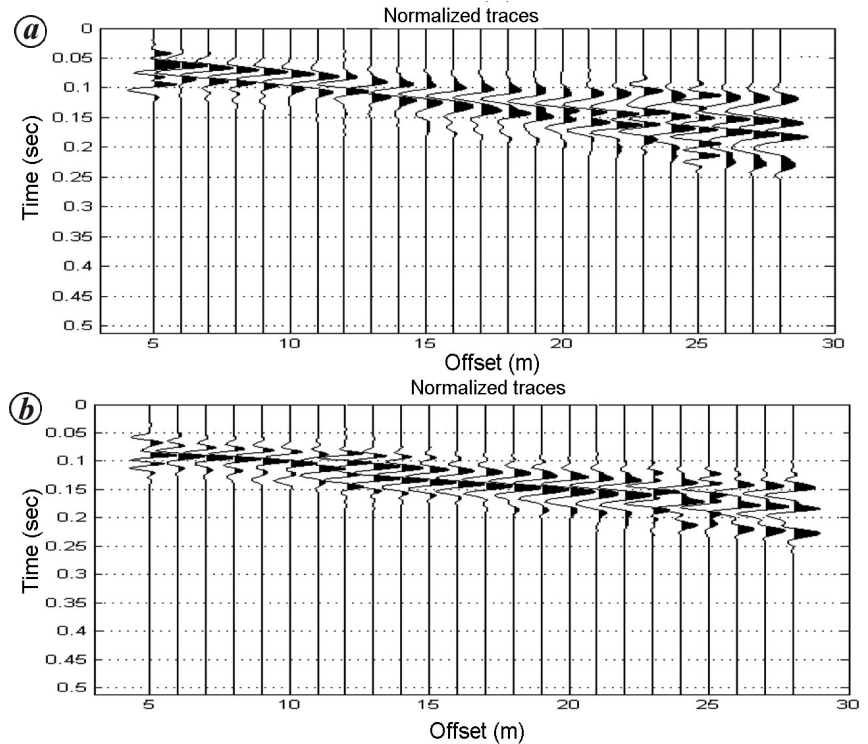


**Figure 1.** Enhanced field data set. *a*, Rayleigh wave data acquired in the field using 24 channel geophone with 4.5 Hz vertical geophones. *b*, Love wave data acquired in the field using 24 channel geophone with 4.5 Hz horizontal geophones.

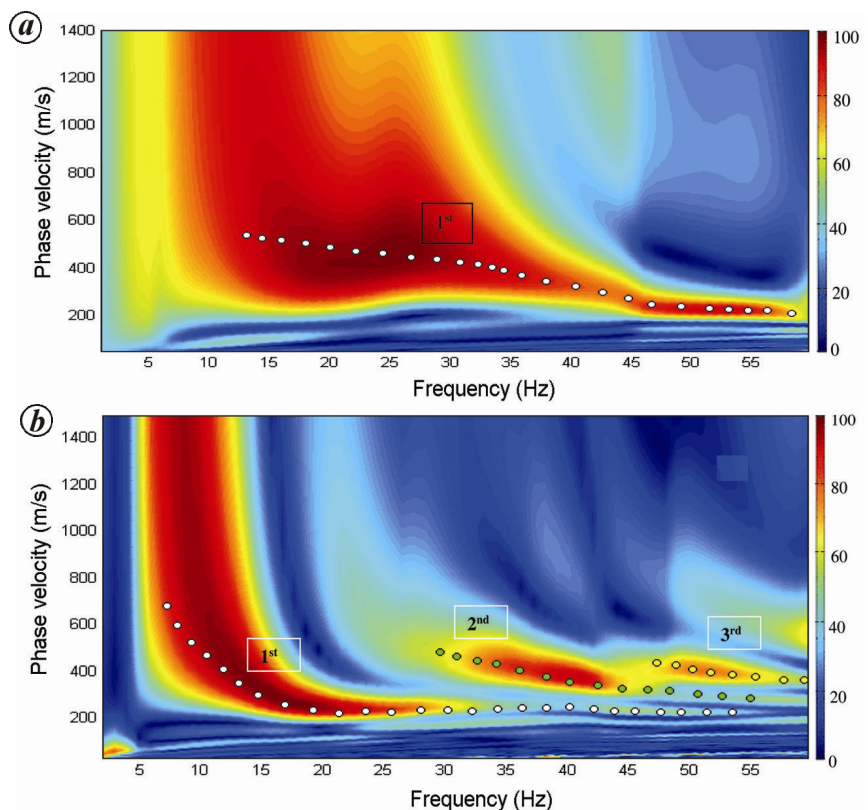


**Figure 2.** *a*, Velocity spectrum of Rayleigh wave where one mode has been picked. *b*, Velocity spectrum of Love wave where three possible modes have been picked.

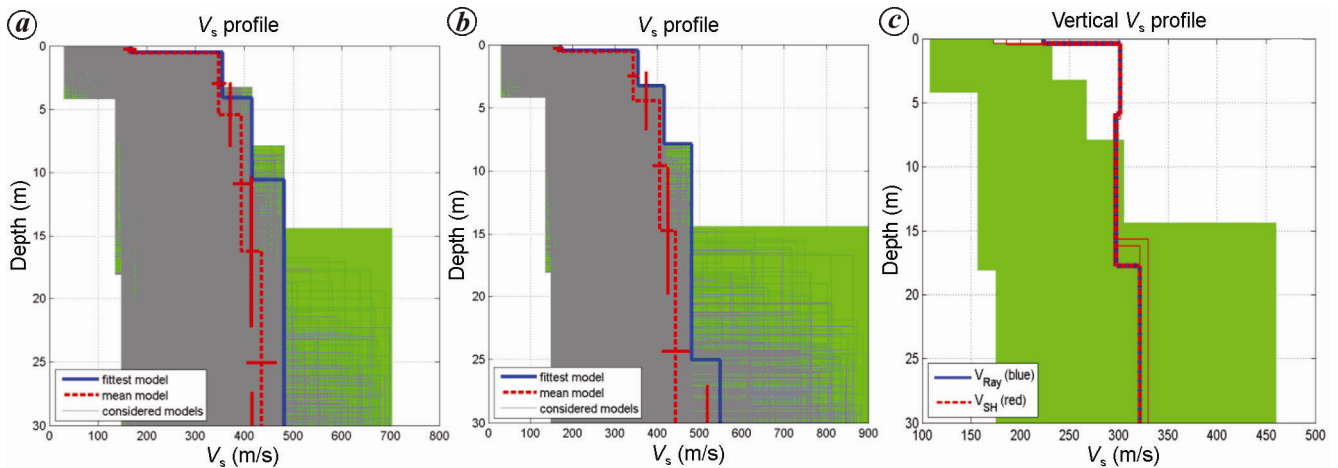


**Figure 3.** All possible generated models of  $V_S$  vertical profiles obtained by (a) inversion of fundamental mode of Rayleigh wave, (b) inversion of three modes of Love wave and (c) joint inversion of fundamental mode of Rayleigh wave and three modes of Love wave.

Rayleigh and Love waves respectively. Figure 2a and b shows the velocity spectrum of Rayleigh and Love waves respectively, with energy distribution among different modes.

Leaving any mode may result in loss of some information; so all possible modes have been exploited. The different modes contain different amounts of energy and information. The fundamental mode of Rayleigh wave has been picked up as shown in Figure 2a, having phase velocity varying from 200 to 520 m/s with a frequency range between 12 and 60 Hz. In Figure 2b, three modes of Love wave are clearly seen. The first mode has been identified having phase velocity varying from 200 to 700 m/s with frequency range between 7 and 54 Hz. The second mode has been identified having phase velocity varying from 250 to 450 m/s having a frequency range 30–55 Hz. The third mode has been identified having phase velocity varying from 350 to 400 m/s having a frequency range 48–58 Hz. The phase velocity variation of the third mode is smooth compared to other modes. However, considering all modes will take a longer time for computing, but results are much better and accurate.

Inversions have been performed assuming five layers using GA<sup>16</sup>, with constant Poisson ratio equal to 0.35. We permitted 0%  $V_S$  anisotropy and 20% variability for  $Q_s$  (quality factor). The number of models and generations has been set to 80. Figure 3a–c shows all possible generated models of  $V_S$  vertical profiles obtained by inversions of (i) fundamental mode of Rayleigh wave, (ii) three modes of Love wave and (iii) joint

inversion of all possible modes of Rayleigh and Love waves respectively. It can be observed from Figure 3 that the best-fitted  $V_S$  vertical profiles are consistent. Figure 4a and b shows the  $V_S$  vertical profiles for Rayleigh and Love waves respectively. Figure 4c shows the  $V_S$  vertical profile generated using joint inversion of Rayleigh and Love waves. In Figure 4, the best models are shown in blue line and the mean models are shown in red line. Joint analysis of all possible modes of Rayleigh and Love wave dispersion has been performed to improve the retrieved vertical shear wave profiles using their complementary information. It is apparent that the possibility of joint analysis of several components has the potential for providing robust interpretation and thus accurate subsurface models<sup>16–18</sup>. It can be observed from Figures 3a and 4a that mean models and best models generated from inversions of Rayleigh wave are deviating from each other both in shallow and deeper part of the vertical  $V_S$  profiles. Similarly, mean models and best models generated from inversions of Love wave do not match both in shallow and deeper parts of the vertical  $V_S$  profiles. However, it is clearly observed from Figures 3c and 4c that both the mean models and best models generated using joint inversion of Rayleigh and Love waves match well in the shallow part up to 17 m. Afterwards, both models have a small deviation, although match better than the other two  $V_S$  vertical profiles (Figure 4a and b). Individual inversions of fundamental mode of Rayleigh wave and three modes of Love wave indicate increasing velocity with depth. However, a relatively low

velocity layer between depth of about 7–17 m has been delineated using joint analysis of fundamental modes of Rayleigh wave and all possible higher modes of Love wave. It is clear that the joint inversion of Rayleigh and Love waves can be effectively utilized to delineate possible vertical  $V_S$  profile anisotropy for shallower strata, while it cannot solve some potential ambiguities for the deep-layer shear velocities<sup>16</sup>.

The main problems in the surface wave analysis are lateral heterogeneities that reduce the resolution of the survey, but if we consider all possible modes of surface waves, ultimately the resolution and accuracy will increase. The non-uniqueness of the solution and complex energy distribution among different modes of Rayleigh and Love waves may create problems which, if not properly considered, can eventually lead to ambiguous or erroneous subsurface models<sup>16</sup>. It is observed from individual inversion of Rayleigh (Figures 3a and 4a) and Love waves (Figures 3b and 4b) that mean models and best models of the vertical  $V_S$  profiles are not properly correlated both in shallow and deeper parts. Whereas, both the mean models and best models of  $V_S$  vertical profiles (Figures 3c and 4c) generated using joint inversion of Rayleigh and Love waves match well in shallow part up to 17 m. Afterwards, both models match with a small deviation which is better than the other two (Figure 4a and b). Individual inversions of Rayleigh and Love waves indicate increasing velocity with depth. However, a relatively low velocity layer between depth of about 7 and 17 m has been delineated using joint analysis of

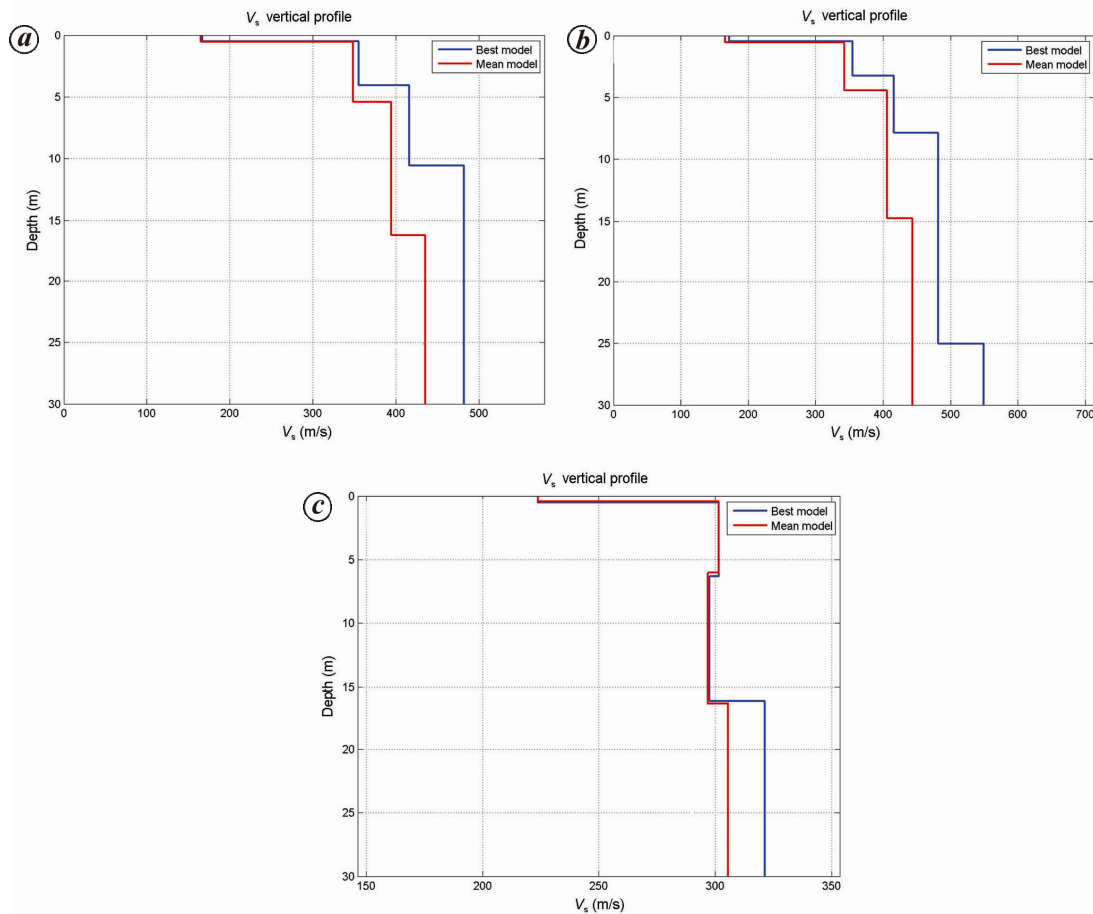


**Figure 4.**  $V_S$  vertical profile obtained by (a) inversion of four modes of Rayleigh wave, (b) inversion of three modes of Love wave and (c) inversion of four modes of Rayleigh wave and three modes of Love wave.

Rayleigh and Love waves. The analysis may not solve ambiguities for the deep-layer shear velocities. However, vertical  $V_S$  profiles for the shallowest part would be improved effectively.

1. Sheriff, R. E., *Encyclopedic Dictionary of Applied Geophysics*, Society of Exploration Geophysicists, Tulsa, 2002, 4th edn, p. 429.
2. Babuska, V. and Cara, M., *Seismic Anisotropy in the Earth*, Kluwer, Academic Publisher, Boston, 1991, p. 217.
3. Xia, J., Miller, R. D., Park, C. B., Ivanov, J., Tian, G. and Chen, C., *The Leading Edge*, 2004, **23**, 753–759.
4. Forbriger, T., *Geophys. J. Int.*, 2003a, **153**, 719–734.
5. Forbriger, T., *Geophys. J. Int.*, 2003b, **153**, 735–752.
6. Hayashi, K. and Suzuki, H., *Explor. Geophys.*, 2004, **35**, 7–13.
7. Herrmann, R. B. and Al-Eqabi, G. I., In *Shear Waves in Marine Sediments*, Kluwer, Academic Publisher, Boston, 1991, pp. 545–556.
8. Xia, J., Miller, R. D., Park, C. B. and Tian, G., *J. Appl. Geophys.*, 2003, **52**, 45–57.

9. Shtivelman, V., *Eur. J. Environ. Eng. Geophys.*, 2002, **7**, 121–138.
10. Xia, J., Xu, Y., Luo, Y., Miller, R. D., Cakir, R. and Zeng, C., *Surv. Geophys.*, 2012, **33**, 841–860.
11. Aki, K. and Richards, P. G., *Quantitative Seismology*, W.H. Freeman and Company, San Francisco, 1980, p. 169.
12. Ivanov, J., Miller, R. D., Xia, J., Steeples, D. W. and Park, C. B., *Pure Appl. Geophys.*, 2005, **162**, 447–459.
13. Ivanov, J., Miller, R. D., Xia, J. and Steeples, D., *Pure Appl. Geophys.*, 2005, **162**, 461–477.
14. Calderón-Macías, C. and Luke, B., *Geophysics*, 2007, **72**(1), 1–10.
15. Luke, B., Calderón-Macías, C., Stone, R. C. and Huynh, M., In Proceedings of the Symposium on the Application of Geophysics to Engineering and Environmental Problems, Environmental and Engineering Geophysical Society, Denver, 2003, pp. 1342–1347.
16. Dal Moro, G. and Ferigo, F., *J. Appl. Geophys.*, 2011, **75**, 573–589.
17. Dal Moro, G., *J. Appl. Geophys.*, 2008, **66**, 15–24.
18. Dal Moro, G., Pipan, M. and Gabrielli, P., *J. Appl. Geophys.*, 2007, **61**, 39–55.

**ACKNOWLEDGEMENTS.** We thank DST, New Delhi for providing funds through a project (SB/S4/ES-640/2012). We also thank Prof. D. C. Panigrahi (Director, ISM, Dhanbad) and Prof. Shalivahan (Department of Applied Geophysics, ISM, Dhanbad) for their keen interest in this study and the anonymous reviewers for their valuable suggestions that helped improve the manuscript.

Received 17 March 2015; revised accepted 24 June 2015

SUNNY KUMAR RANJAN<sup>1</sup>  
S. K. PAL<sup>1,\*</sup>  
K. K. K. SINGH<sup>2</sup>

<sup>1</sup>Department of Applied Geophysics, Indian School of Mines, Dhanbad 826 004, India

<sup>2</sup>CSIR-Central Institute of Mining and Fuel Research, Dhanbad 826 015, India

\*For correspondence.  
e-mail: sanjitism@gmail.com